ISSN: 0067-2904

The Relationships of Dust and Total Masses of Luminous Infrared Galaxies with Their Far Infrared and Total Luminosities Using Two Methods of Distance Measurements

Farah Z. Shaker*, Al Najm M. N.
Department of Astronomy and Space, College of Science, University of Baghdad, Baghdad, Iraq

Received: 1/2/2023 Accepted: 5/7/2023 Published: 30/7/2024

Abstract

This research aims to determine the nature of the relationships among luminous infrared galaxies (LIRGs) by using different methods of distance measurement (distance modulus "dm" and luminosity distance "dl"). We used data from the following sources: NASA Extragalactic Database (NED) and the HYPERLEDA database, where this data was used to study the nature of the relationships and the extent to which they relate to each other. The program (statistica-win-program) was employed, which helped us know the strength of the association between the variables. The results of the statistical analysis showed that there was a strong correlation between dust mass ($M_{dust\ dm}$ & $M_{dust\ dl}$) and luminous infrared (L_{FIRdm}, L_{IRdm}) & (L_{FIRdl}, L_{IRdl}), where the partial correlation coefficient was equal to (R≃0.7) and the slope was linear. There was also a positive correlation between (L_{FIRdm}, L_{FIRdl})& (T_d) where the partial correlation coefficient was (R≃0.4) with a linear slope. The relationship between (L_{IR})& (T_d) was a positive relation in the modulus distance case (dm), where its correlation was equal to (R≃0.4), but in another case (luminosity distance), the relation was very weak, and the correlation was (R≃0.2). The relationship between total masses (M_i) & ($L_{FIRdm,\ dl}$) in both cases of distance (dm) & (dl) was good, and the partial correlation coefficient was equal to (R≃0.4) with a linear slope. The relationship between (L_{IR}) & (M_i) in both cases of distance was also positive, and the partial correlation coefficient was equal to (R≃0.3). There was an inverse relationship between the ratio fluxes (F100/F60) & (T_d), as well as a very tight partial correlation coefficient, which was equal to (R≃-0.9) with a slope of (-1).

Keywords: luminous infrared galaxies; distance scale; dust extragalactic; infrared emission; partial correlation.

علاقات الكتل الغبارية و الكلية لمجرات الأشعة تحت الحمراء اللامعة مع ضيائيتها تحت الحمراء البعيدة والكلية باستخدام طريقتين لقياسات المسافة

فرح زياد شاكر* ، محمد ناجي ال نجم
قسم الفلك والفضاء، كلية العلوم، جامعة بغداد، بغداد ، العراق

الخلاصة:

يهدف هذا البحث الى تحديد طبيعة العلاقات بين مجرات الاشعة تحت الحمراء اللامعة (LIRGs) باستخدام طرائق مختلفة لقياس المسافة (معامل المسافة "dm" والمسافة الضيائية "dl"). استخدمت قاعدة البيانات في هذا

* Email: farahzeyad9997@gmail.com

البحث من المصادر التالية: قاعدة بيانات NASA Extragalactic Database (NED) و HYPERLEDA حيث تم استخدام هذه البيانات لدراسة طبيعة العلاقات ومعرفة مدى الارتباط فيما بينها. تم استخدم برنامج (statistic–win–program) الذي ساعدنا على معرفة قوة الارتباط بين المتغيرات. بينت نتائج التحليل الاحصائي وجود علاقة ارتباط قوية مابين كتلة الغبار ($M_{dust\ dm}$و$M_{dust\ dl}$) والاشعة تحت الحمراء اللامعة البعيدة والكلية ($L_{FIR\ dm}$, $L_{IR\ dm}$) و($L_{FIR\ dl}$, $L_{IR\ dl}$) حيث كان معامل الارتباط يساوي ($R\simeq0.7$) والميل خطي .هناك علاقة ايجابية بين الاشعة تحت الحمراء اللامعة الكلية ($L_{FIR\ dm}$, $L_{FIR\ dl}$) ودرجة حرارة الغبار (T_d) حيث كان معامل الارتباط الجزئي يساوي ($R\simeq0.4$) والميل خطي . اما بالنسبة لعلاقة الاشعة تحت الحمراء اللامعة البعيدة مع درجة حرارة الغبار فقد كانت علاقة ايجابية مع نوع المسافة (dm) حيث ان معامل الارتباط الجزئي كان يساوي ($R\simeq0.4$) والميل خطيا اما في حالة نوع المسافة الاخر (dl) فقد كانت علاقة ضعيفة جدا حيث ان معامل الارتباط الجزئي يساوي ($R\simeq0.2$). العلاقة بين الكتلة الكلية (M_i) والاشعة تحت الحمراء اللامعة الكلية ($L_{FIRdm,\ dl}$) وفي حالتي المسافة المختلفة (dm)و(dl) فقد كانت هناك علاقة ايجابية ذات معامل ارتباط جزئي يساوي ($R\simeq0.4$) وبميل خطي. اما علاقة الاشعة تحت الحمراء اللامعة البعيدة (LIR) والكتلة الكلية (M_i) فقد كانت علاقة ايجابية ايضا ذات معامل ارتباط يساوي ($R\simeq0.3$) وميلاً خطياً.هناك علاقة عكسية مابين نسبة الفيض (F100/F60) و(T_d) بالاضافة الى معامل ارتباط جزئي قوي جداً والذي يساوي ($R\simeq-0.9$) والميل مساوي (-1).

1. Introduction

Luminous Infrared Galaxies (LIRGs) are considered as one of the most important discoveries from extragalactic space, where the luminosity of these galaxies is about 10^{11} $L_{\odot}$. They are abundant in the Universe. When compared with other galaxies, such as starburst galaxies, Seyfert galaxies, and quasars, it was found that the energy emitted by IR radiation is much greater than all other wavelengths, as the luminosity in them is equivalent to 100 billion times the luminosity of the sun [1]. The first survey of the sky using IR emission was conducted by the infrared astronomical satellite (IRAS) in 1983. It completed its mission in 10 months, during which more than 350000 sources of infrared were observed at wavelengths 12, 25, 60, and 100 micrometers(μm). The mission carried out by IRAS was considered as one of the successful missions, as this success led to an interest in this type of telescopes and worked to develop them until reaching the James Webb Telescope, which was launched on December 25, 2021, which was one of the space observatories that surpassed all other telescopes in terms of accuracy [2].

Several studies focused on luminous infrared galaxies. The researchers (1991) took 90 samples from a luminous infrared galaxy, and they studied mass and its relationship to L_{FIR}. This led to the conclusion that galaxies with large FIR luminosity are giant ones, whether taken under the aspect of their total mass, dimension, or blue luminosity. This relatioship increases with increasing FIR luminosity [3]. In 1996, the scientists found that one of the most important stages in the formation of quasi-stellar objects and powerful radio galaxies are ultra-luminous infrared galaxies, and they also enter into the formation of the hearts of elliptical galaxies as an initial stage [1]. The authors (2005) tested many samples and found a total difference between luminous infrared galaxies and ultra-luminous infrared galaxies[4]. After comparing the luminous infrared galaxies (LIRGs) with other types of distant and local galaxies, the analyzers (2012) found that there was a vast difference in terms of density between them, as the local bright infrared galaxies are located in more dense areas than the distant ones [5]. The researchers (2016), after the morphological classification was conducted for 89 samples of luminous infrared galaxies, using non-parametric coefficients and comparing them morphologically as a function of wavelength, found that the morphological trace is directly proportional to the wavelength of the band from B to H [6]. Al Najm (2020) investigated the

amount of cold gas (MHI, MH2), dust abundance (M_{dust}), the cold temperature of dust (T_d), and brightness in far-infrared to CO line radiant energy of the extragalactic sample. His findings showed that far-infrared emission has a strong association with all parameters, which demonstrates the existence of a recent star-burst, which is in turn a significant indicator of stellar evolution activity [7].

2. Data collection for sample observations

The Lyon-Meudon Extragalactic Database (HYPERLEDA) is a database of galaxies. LEDA originally contained information of more than 60 parameters for about 100,000 galaxies, and now includes information on over 3 million celestial objects, of which about 1.5 million are galaxies. We have studied apparent and absolute magnitudes (m_{btc}, M_B), the apparent maximum rotation speed of the gas at the level of 20% (W20%), their apparent diameters d_{25}, and their shapes. We also used NASA/IPAC (NED), an online database for astronomers that collects and links information about extragalactic objects like galaxies, quasars, radio, X-ray, and infrared sources, etc. This site has helped us get many parameters (for example, the redshift of galaxies (z), infrared fluxes in different bands at near, medium, and far F12, F25, F60, plus F100 in unit Jansky (Jy). In this research, 134 galaxies were selected from the literature [8-16], and the data were collected from NED and HYPERLEDA.These sites have helped us get many parameters, as seen in Table (1) in which:

Column 1 presents the number of objects, column 2 presents the name of the galaxy, column 3 devotes itself to the morphological classification, column 4 tackles the apparent diameters, column 5 gives the redshift of galaxies, column 6 presents the inclination, column 7 lists the apparent maximum rotation speed of the gas at the level of 20%, columns 8, 9, 10 and 11 present the infrared fluxes in different bands at near, medium, and far F12, F25, F60, plus F100 in unit Jansky (Jy), respectively, column 12 refers to the apparent magnitude m_{btc} , and column 13 presents the apparent size.

Table 1: The data obtained from NASA/IPAC extragalactic archive (NED), and the Lyon-Meudon Extragalactic Database website (HYPERLEDA).

NO.	Name of galaxy	Morphological Type	Log d25 arcmin	z	Incl (i)	W20% Km/s	F12 Jy	F25 Jy	F60 Jy	F100 Jy	m_{btc} mag	MB
1-	NGC 23	Sa	1.19	0.01523	40.5	443.1	0.66	1.29	9.03	15.66	12.51	-21.45
2-	NGC5257	SABb	1.17	0.02267	62.1	534.6	0.52	1.18	8.1	13.63	13.04	-21.96
3-	NGC5258	SBb	1.17	0.01523	34.2	444	0.25	0.78	3.94	7.27	13.5	-21.5
4-	NGC 877	SABc	1.28	0.01306	41.1	438.5	0.84	1.41	8.82	25.56	11.82	-21.93
5-	PGC049264	SABb	1.03	0.03304	60.2	181	0.29	0.79	6.27	10.71	15.99	-19.86
6-	NGC 958	SBc	1.4	0.01915	78	601.7	0.62	0.94	5.85	15.08	11.86	-22.6
7-	NGC 3683	SBc	1.24	0.0057	69	379	1.19	1.48	13.87	29.3	12.24	-20.26
8-	UGC 1845	Sab	0.9	0.03304	82.3	295.1	0.35	0.883	9.919	15.51	14.32	-19.44
9-	UGC 02982	SABa	0.89	0.01514	63.7	430.5	0.57	0.83	8.391	16.82	13.31	-20.94
10-	UGC 3351	Sab	1.24	0.01486	90	508.2	0.55	0.86	14.45	29.26	13.99	-20.01
11-	NGC 2369	Sa	1.48	0.01081	90	542.1	0.7089	2.205	19.31	38.31	12.13	-20.73
12-	NGC 992	SBc	0.9	0.01378	42.8	108	0.56	1.76	11.4	16.72	14.64	-19.08

13-	NGC6090	Sab	0.64	0.0293	71	231.7	0.29	1.22	6.48	9.34	13.96	-21.67
14-	NGC 2388	Sb	0.94	0.01379	52.6	464.5	0.69	1.19	16.74	25.64	14.09	-19.84
15-	MCG +02-20-003	S0-a	0.95	0.01657	75.7	389.9	0.26	0.73	8.81	12.8	14.72	-19.55
16-	NGC 3110	SBb	1.27	0.01686	64.8	442.6	0.59	1.13	11.68	22.27	12.34	-21.96
17-	NGC 3256	Sbc	1.52	0.00935	48.2	271.3	3.57	15.69	102.36	114.31	11.29	-21.59
18-	NGC 3690	Sm	1.38	0.01041	43.6	577	3.9	24.51	121.64	122.45	11.41	-22.06
19-	NGC 828	Sa	1.46	0.01785	44.8	556	0.72	1.07	11.46	22.83	12.74	-21.7
20-	NGC 5135	Sab	1.38	0.01369	24.8	221.8	0.63	1.783	16.68	30.97	12.47	-21.37
21-	UGC 08739	SBbc	1.28	0.01679	87.5	174	0.35	0.42	5.79	15.89	13.42	-21
22-	NGC5653	Sb	1.2	0.0119	35	129	0.63	1.37	10.57	23.03	12.69	-20.85
23-	NGC 834	Sb	1.02	0.01532	65.8	258.2	0.41	0.84	6.65	12.77	13.14	-21.03
24-	NGC 5743	Sb	1.11	0.01374	75	571.5	0.59	0.75	5.21	9.78	12.85	-21.01
25-	NGC 5936	SBb	1.07	0.0133	19.3	217	0.48	1.47	8.73	17.66	12.82	-21.14
26-	NGC 5990	SABa	1.2	0.01277	57.5	406.4	0.6165	1.6	9.59	17.14	12.24	-21.18
27-	NGC 6156	Sc	1.27	0.01089	33.3	235	1.23	2.71	20.9	32	11.46	-21.82
28-	NGC 6701	Sa	1.15	0.01323	17.3	314.8	0.55	1.32	10.05	20.05	12.57	-21.4
29-	NGC 7469	Sa	1.14	0.01627	30.2	395.4	1.63	5.7	23.13	40.15	12.48	-21.77
30-	NGC 7591	SBbc	1.21	0.01654	66.9	390	0.323	1.23	7.87	14.87	12.86	-21.28
31-	NGC 7679	S0-a	1.09	0.01715	59.3	449	0.5	1.12	7.4	10.71	13.02	-21.35
32-	NGC 7769	Sb	1.26	0.01405	73.2	88	0.52	5.21	4.339	13.58	11.55	-22.42
33-	NGC7817	Sbc	1.52	0.01532	90	434	0.66	0.61	5.19	16.78	11.41	-20.94
34-	NGC 7771	Sa	1.4	0.01446	66.7	659.1	0.99	2.17	18.99	37.42	12.3	-21.72
35-	NGC 6621	Sb	1.33	0.02065	70.8	459.2	0.31	1.02	7.02	12.19	12.61	-22.27
36-	UGC 2608	SBb	0.98	0.02334	36.5	319	0.44	1.45	8.166	11.27	13.5	-21.56
37-	UGC03973	Sb	1.13	0.02221	36.7	197	0.3062	0.7625	1.503	2.363	13.14	-21.84
38-	NGC7674	SBbc	1.05	0.02903	26.7	344.3	0.68	1.896	5.36	8.146	13.59	-21.95
39-	NGC520	Sa	1.61	0.00761	75.7	219.8	0.9	3.22	30.87	47.76	11.67	-20.75
40-	NGC660	Sa	1.66	0.00283	78.8	319.9	2.88	7.3	65.52	114.74	11.26	-19.25
41-	NGC 4303	Sbc	1.84	0.00522	18.1	239	3.28	4.9	23.46	78.74	10.02	-20.43
42-	NGC1055	SBb	1.84	0.00332	62.7	87	2.24	2.84	23.37	65.26	10.84	-20.6
43-	IC0860	SBab	0.98	0.01291	54.6	658	0.9	1.34	17.66	18.09	14.14	-19.7
44-	NGC1134	Sb	1.35	0.01214	77.2	450.8	0.55	0.92	9.09	16.43	11.75	-21.19
45-	NGC 3198	Sc	1.81	0.0022	77.8	313.2	0.71	1.08	7.47	18.52	9.94	-20.79
46-	UGC2982	SABa	0.89	0.0177	63.7	426.6	0.57	0.83	8.38	16.86	13.31	-20.94
47-	NGC1797	Sba	1.08	0.01487	53.4	380.2	0.33	1.35	8.264	12.76	13.84	-20.21
48-	NGC6814	SABb	1.49	0.00522	85.6	114.9	0.92	0.5986	6.53	19.67	10.35	-21.57
49-	NGC6835	Sba	1.44	0.00541	90	190.1	0.65	1.37	11.16	16.82	12.2	-19.77
50-	UGC12150	S0-a	0.95	0.02139	61.4	479	0.37	0.791	8.166	15.58	14.43	-20.51
51-	NGC 157	SABb	1.57	0.0055	61.8	327.3	1.61	2.17	17.93	42.43	10.4	-21.81

52-	NGC 4593	Sb	1.83	0.00831	34	362.2	0.25	0.00831	3.052	5.947	11.65	-21.4
53-	NGC 7213	Sa	1.68	0.00584	39.1	210	0.6063	0.7421	2.666	8.177	10.81	-21.05
54-	NGC7678	Sc	1.31	0.03363	43	360	0.63	1.16	6.98	14.84	12.05	-21.21
55-	NGC 3393	SBa	1.29	0.01164	30.9	243.1	o.131	0.7528	2.251	3.378	12.6	-21.01
56-	NGC 4151	Sab	1.46	0.00333	42	137.1	1.968	4.87	6.46	8.88	11.09	-17.3
57-	NGC 5100	Sb	0.97	0.03191	46.9	390	0.21	0.2654	2.164	4.605	14.48	-21.28
58-	NGC 5506	SABa	1.46	0.00608	90	322	1.48	4.29	8.55	8.87	12.05	-20.2
59-	NGC1614	SBc	1.1	0.01594	41.8	142	1.38	7.5	32.12	37	12.71	-21.4
60-	Mrk 796	S0-a	0.79	0.02156	51.2	338.1	0.2026	0.7483	3.457	5.416	14.9	-20.02
61-	NGC 7212	Sb	1.13	0.02663	76.4	591	0.1955	0.769	2.885	4.895	13.96	-21.39
62-	NGC 1122	SABb	1.13	0.01201	65.3	440.6	0.2015	0.2607	1.996	4.937	12.06	-21.63
63-	NGC 988	Sc	1.64	0.00504	69.1	256	0.2274	0.2253	2.331	8.075	10.11	-20.87
64-	IC 2810	SBAb	1.01	0.03401	75.2	439	0.14	0.62	5.1	10.98	14.6	-21.29
65-	NGC 4418	SABa	1.15	0.00709	68.1	160	0.99	9.67	43.89	31.94	13.42	-19.09
66-	NGC 0034	S0-a	1.06	0.01962	90	514	0.35	2.39	17.05	16.86	13.95	-20.68
67-	Mrk 739	Sb	0.85	0.02985	37.4	380	0.1603	0.3093	1.26	2.408	14.29	-21.31
68-	Mrk 915	Scd	1.01	0.02411	67	375.8	0.12	0.252	0.4578	1.007	13.84	-21.27
69-	NGC 2623	Sb	1.38	0.01851	83	95	0.21	1.81	23.47	25.88	13.06	-21.86
70-	NGC 3256	Sbc	1.52	0.00935	48.2	306	3.57	15.69	102.63	115.3	11.29	-21.59
71-	NGC 3690	Sm	1.38	0.01041	43.6	577	3.9	24.14	113.05	111.4	11.41	-22.06
72-	UGC 08387	Sm	0.9	0.02306	61.4	279.3	0.25	1.42	17.04	24.38	14.24	-20.85
73-	MCG -02-08-039	Sa	1.09	0.02411	55.8	445.7	0.2004	0.4758	0.5081	2.4	13.99	-21.55
74-	VV283	SBb	0.76	0.03748	33.1	332.7	0.3	0.47	5.25	8.06	15.14	-20.96
75-	NGC 4507	Sab	1.14	0.0118	32.5	258.4	0.4566	1.502	4.31	5.399	12.48	-20.98
76-	NGC 6240	S0-a	1.34	0.02431	72	616.6	0.59	3.55	22.86	26.49	13.26	-21.92
77-	NGC 4194	SBm	1.22	0.00834	52.6	148.9	0.99	4.51	3.16	9.46	12.58	-20.49
78-	NGC 4704	SBbc	1	0.02715	20	50	1.6	0.473	1.757	2.563	14.36	-20.87
79-	NGC 5347	Sab	1.21	0.0079	45.3	121.9	0.3085	0.9625	1.424	2.644	13.16	-19.75
80-	NGC 7714	Sb	1.34	0.00933	45.1	220.8	0.47	2.88	12.7	12.46	12.52	-20.51
81-	NGC 3049	SBb	1.32	0.00486	58	211.8	0.16	0.44	2.95	4.24	13.02	-18.32
82-	NGC 1667	SABc	1.27	0.01526	39.8	389.9	0.42	0.71	6.27	14.92	15.77	-21.81
83-	UGC 9944	Sbc	1.14	0.02453	79.6	418	0.25	0.6	1.34	2.07	13.82	-21.43
84-	UGC 6100	SA	0.9	0.02941	52.2	375	0.1453	0.2018	0.5743	1.498	13.83	-21.74
85-	UGC 12348	Sba	1.11	0.02538	90	94	0.1088	4.2	9.6	15.57	14.68	-20.55
86-	NGC 024	Sc	1.79	0.00185	70.1	168	0.27	0.1632	1.261	6.723	11.3	-18.02
87-	IIzw096	S0-a	0.79	0.0361	71.4	412.1	0.2545	2.394	13.28	11.76	14.65	-21.38
88-	NGC 337	SBcd	1.47	0.0055	50.6	272	0.222	0.76	9.07	20.11	11.18	-20.23
89-	NGC 0628	Sc	2	0.00219	19.8	52.4	2.45	1.9	20.86	65.64	9.35	-20.68

90-	NGC1512	Sa	1.93	0.00299	68.3	272.3	0.2237	0.2396	3.4	11	9.16	-19.66
91-	NGC 2798	Sa	1.38	0.0058	84.9	355	0.76	3.21	19.29	29.69	12.5	-19.66
92-	NGC 2915	Sbab	1.26	0.00156	62.2	176	0.25	0.934	0.899	1.66	11.7	-16.46
93-	NGC 5194	SABb	2.14	0.00153	32.6	139	7.21	9.56	98.8	221.21	8.34	-21.33
94-	NGC 3621	SBcd	1.98	0.00224	67.6	293	3.53	4.44	29.32	77.34	9.06	-20.08
95-	NGC 3627	Sb	2.01	0.00241	67.5	376.1	4.82	7.72	66.31	179	9.09	-21.21
96-	UGC 3374	SBbc	1.35	0.02046	27.3	321	0.41	1.948	3.005	4.235	12.49	-22.29
97-	NGC 3094	Sba	1.13	0.00802	46.1	266.1	0.82	2.89	10.88	13.89	13.14	-19.88
98-	NGC 3190	Sa	1.56	0.00437	87.8	271	0.34	0.47	3.16	9.46	11.4	-20.53
99-	NGC 6946	SABc	2.06	0.00013	18.3	233.3	12.11	20.7	129.78	290.69	8.23	-20.9
100-	NGC 5713	SABb	1.39	0.00628	48.2	216	1.47	2.84	20.69	37.28	11.18	-21.21
101-	Mrk463	Sc	1.03	0.0508	59	200	0.5098	1.576	2.184	1.924	13.7	-23.08
102-	NGC 3938	Sc	1.73	0.00269	17.6	115	0.9	1.23	9.18	27.5	10.74	-20.12
103-	Arp220	Sm	1.04	0.0184	57		0.4837	8	113.35	115.29	13.38	-21.21
104-	NGC 418	Sc	1.3	0.01904	50.4	266.6	0.1297	0.1984	1.494	4.281	12.72	-21.8
105-	NGC 4236	SBd	2.37	0	90	182	0.11	0.57	3.98	10.02	9.02	-19.2
106-	NGC 633	SBb	1.04	0.01731	31.5	243.2	0.22	0.72	2.01	2.32	13.33	-20.95
107-	NGC 4254	Sc	1.7	0.00803	20.1	283.8	3.67	4.38	25.3	76.01	10.17	-20.6
108-	NGC 4451	Sab	1.74	0.00653	48.8	163	0.1085	1.2	1.343	6.952	10.46	-19.12
109-	NGC 4736	SABc	1.89	0.00103	31.8	244.9	5.07	6.13	71.54	20.69	8.54	-19.67
110	IC 860	SBab	0.98	0.01291	54.6	658	0.14	1.34	18.61	18.66	14.14	-19.7
111-	NGC 2339	Sbc	1.38	0.00752	52.6	429	0.59	2.4	17.6	31.82	11.77	-20.67
112-	IC 5179	Sbc	1.01	0.01141	62.2	409.3	1.18	2.4	19.39	37.29	12.03	-21.31
113-	IC 4734	SBbc	1.12	0.01605	57.2	361.6	0.38	1.33	14.04	25.31	13.42	-20.73
114-	NGC 4679	SBc	1.39	0.01549	72.4	422.8	0.2479	0.2192	2.244	7.098	13.4	-20.46
115-	NGC 4559	Sc	2.02	0.00398	64.8	247.2	0.35	0.301	1.87	4.82	9.6	-19.67
116-	UGC 3608	Sc	1.17	0.02165	48.4	187.1	0.41	1.2	8.05	11.33	12.97	-21.95
117-	NGC 1068	Sb	1.79	0.00379	34.7	299.9	39.84	87.57	196.37	257.37	9.47	-20.64
118-	NGC 2342	Sc	1.07	0.01765	45.1	411.1	0.46	1.64	7.73	16.66	12.77	-21.62
119-	N6090	Sab	0.64	0.0293	71	357.3	0.26	1.24	6.48	9.41	13.96	-21.67
120-	NGC 4725	SABa	1.99	0.00403	45.4	393.6	0.32	0.2	4.18	20.79	9.68	-20.73
121-	Arp 193	Sm	0.9	0.02306	61.4	279.3	0.25	1.362	17.04	24.38	14.24	-20.85
122-	NGC 4536	SABb	1.85	0.00603	73.1	342	1.6	3.9	30.26	44.51	10.27	-20.54
123-	Mrk 331	Sa	0.93	0.01814	43.7	100.9	0.52	3.02	18	22.56	14.29	-20.23
124-	NGC 5195	Sba	1.74	0.00152	40.5	239	0.72	1.02	15.22	31.33	10.26	-19.14
125-	NGC 6000	SBbc	1.28	0.00732	30.7	308.7	1.48	5.35	35.64	54.94	12.17	-20.39
126-	NGC 5033	Sc	1.99	0.00152	64.4	464.5	1.38	1.99	16.2	50.23	10.08	-20.76
127-	NGC 1433	Sba	1.79	0.00359	67.4	184	0.2366	0.2303	3.492	14.23	10.42	-19.22

128-	UGC1845	Sab	0.9	0.01514	82.3	295.1	0.35	1.07	10.31	15.51	14.32	-19.44
129-	NGC 5055	Sbc	2.07	0.00167	54.9	397.2	5.35	6.36	30.15	139.82	8.89	-20.89
130-	IC 4710	Sm	1.54	0.00247	34.1	71	0.1143	0.1213	0.9824	2.571	12	-17.34
131-	NGC 4102	SABb	1.47	0.00282	58.7	349.8	1.77	6.76	46.85	70.29	11.62	-19.67
132-	NGC 7552	Sab	1.59	0.00536	23.6	257	3.49	11.92	78.38	102.92	11.06	-20.57
133-	NGC 7793	Scd	2.02	0.00076	63.5	191.1	1.32	1.67	18.14	54.07	9.19	-18.67
134-	NGC 4818	SABa	1.63	0.00355	85.9	316.2	0.96	4.4	20.12	26.6	11.26	-19.01

2. Calculations, statistical analyses, and results

In this section, the following parameters have been determined for the sample of galaxies considered in this study.

Far infrared luminosity L_{FIR}: In general, the relationship was used to calculate the logarithm of the far infrared luminosity of galaxies (L_{FIR}) in solar units using the following formula [3]:

$$\text{Log}\left[\frac{L_{FIR}}{L_{\odot}}\right] = 5.5954 + 2\text{LogD} + \text{Log}[2.58\text{F}_{60} + \text{F}_{100}] \qquad (1)$$

Where (F_{60}, F_{100}) refer to IRAS flux densities at 60 and 100 micrometers, and D is the extragalactic distance, where both types of distance include (dm & dl)where this equation was applied in both cases .

Additionally, the following formula has been used to calculate the logarithm of the total infrared luminosity L_{IR} at fluxes (12, 25, 60, and 100) [3]:

$$\text{Log}\left[\frac{\text{L}_{\text{IR}}}{\text{L}\odot}\right] = 5.5378 + 2log\text{D} + \log\left[12.66F_{12} + 5.00F_{25} + 2.55F_{60} + 1.01F_{100}\right. \qquad (2)$$

Where D is applied in both cases of extragalactic distances (dm & dl).

Dust temperature T_d: Is one of the important characteristics of galaxies, it is directly related to the rate of star formation and plays a vital role in the thermodynamics of interstellar clouds. It is also involved in astrochemical studies [17]. This relationship is used to calculate (T_d) [7, 18]:

$$\text{T}_\text{d} \approx 49\left(\frac{F_{60}\mu m}{F100\mu m}\right)^{0.4} \qquad (3)$$

Here, the dust temperature is measured in Kelvins and the fluxes (F60 μm and F100 μm) in Jansky.

Dust mass of galaxies (M_{dust}) : Spiral galaxies consist of stars, dust, and gas in varying proportions. Dust is present in small proportions in galaxies, but it plays an important role in explaining how light escapes from galaxies because dust grains can absorb and scatter light [17,19]. According to recent studies, tidal interaction causes galaxies to release interstellar gases as well as dust [20]. To calculate the mass of dust, the following formula has been used [7]:

$$\text{M}_{\text{dust}}\left(\text{M}_{\odot}\right) = 4.78\text{F}_{100}(\text{Jy})\text{D}^2\left\{\text{e}^{\frac{144}{\text{Td}}} - 1\right\} \qquad (4)$$

Where D is applied in both cases of extragalactic distances (dm&dl).

Total mass of galaxies (Mi): Determining the total mass of galaxies is one of the most difficult parameters for astronomers, as there are usually many methods found to calculate the mass, such as the velocity dispersion method, and the average mass method through the application of the Virial theorem, but it is known that astronomers are always looking for better methods that are considered easier to give us higher initial calculations [21]. The following relationship has been used to calculate the total mass [3]:

$$\mathrm{LogMi}(\mathrm{M}_{\odot}) = 4.4771 + \mathrm{Log}\,\mathrm{A}_0 + 2\mathrm{Log}\,\Delta\mathrm{v}_0 \qquad (5)$$

To apply the total mass equation, the linear diameter of the galaxies ($A_\circ$) must be found, where ($A_\circ$) is the distance between the two opposite sides [22], and it can be found through this equation [3]:

$$\mathrm{A}_\circ = 0.290887 * \mathrm{d}_{25} * \mathrm{D} \qquad (\mathbf{6})$$

Where d_{25} is the diameter measured by an observer at a specific distance from the object, called the apparent diameter in (arcmin) units [23] ,and D includes both types of extragalactic distances (dm &dl).
$\Delta v_\circ$ is the observed line width, and it can be calculated using the following relationship [3]:

$$\Delta\mathrm{v}_\circ = \frac{\mathrm{W20}}{\mathrm{sini}} \qquad \mathbf{(7)}$$

Where w_{20} is the maximum rotation speed of gas at level 20% and the inclination (i) is one of the elements that determine the directions and shapes of astronomical bodies, as each celestial body has its own inclination angle [24].

In equations 1, 2, 4, and 6, the symbol D denotes the luminosity distance of luminous infrared galaxies (LIRG) , which has been calculated in two ways in this work: distance modulus dm and luminousity distance dl.

Distance modulus (dm): Is the difference between apparent magnitude and absolute magnitude. This distance can be measured using the following formula [25]:

$$\mathrm{m_{btc}} - \mathrm{M_B} = 5\log\mathrm{dm} + 25 \qquad (8)$$

The above equation can be rearranged in order to measure the luminosity ditsnace (dm) from distance modulus as follows:

$$\mathrm{dm(Mpc)} = 10^{(\mathrm{m_{btc}} - \mathrm{M}_B - 25)/5} \qquad (9)$$

Where the absolute magnitude M_B is the star's magnitude resulting from its position at a distance of 10 parsecs from the Earth , and the apparent magnitude m_{btc} refers to the brightness produced by stars or galaxies that the observer measures when they are at a certain distance from the celestial sphere [26].

Distance luminousity (dl): This type of distance tells us how far the light travels to reach us [27]. This relationship is used to calculate it [25]:

$$\mathrm{dl(Mpc)} = \frac{\mathrm{cz}}{H_\circ}\left\{1 + \mathrm{z}(1 - \mathrm{q}_\circ)^{\frac{1}{2}}/1 + \mathrm{q}_\circ\mathrm{z}(1 + 2\mathrm{q}_\circ\mathrm{z})^{\frac{1}{2}}\right\} \qquad (10)$$

Where $H_\circ$ is the Hubble constant, which tells us about the speed with which the universe expands and is used to approximately calculate the universe's age. Its values range from 68 km/s/Mpc to 74 km/s/Mpc [28]. In this research, we used the value $H_0 \approx 68.7$ Km/s/Mpc, c is the speed of light ($3x10^5$ km/s), and $q_\circ$ is the deceleration coefficient, which is a measure of

cosmic expansion, but without dimensions, and its value in this equation was equal to ½. Throughout the present work, we have employed cosmological parameters with the following quantities $\Omega_M = 0.3$, *and* $\Omega_\Lambda = 0.7$ [29, 30]. In this equation, the redshift z is one of the methods used to infer the movement of distant celestial bodies, as it is known that when the body is redshifted, it moves away from us, but if it is blueshifted, it approaches us. Therefore, the redshift is an example of the Doppler effect [31, 32].

The purpose of this study is to determine the nature of the relationships between dust and total masses, as well as the bolometric infrared photometry of luminous infrared galaxies using various extragalactic distance measurement methods, where photometry is considered one of the most important basics for the study of astronomical phenomena, such as the study of galaxies [33, 34]. A group of galaxies (134) were taken from the luminous infrared galaxies of the spiral type; we took the basic information that we needed from the (HYPERLEDA) and (NED) websites. The previously mentioned mathematical equations were applied, and we input all the data we obtained into the statistical program to find out the nature of these relationships. The statistical program is considered one of the popular programs that are used to see if there is a correlation between variables in this study. Partial correlation coefficient (R) values range from [+1, -1]. If the value is positive +1, the strength of the correlation between the two variables is high, and the correlation between the two variables is weak when the value of the partial correlation coefficient is zero or close to it [35]. The nature of the relationships was determined using different measurement methods. The first one was the luminosity distance (dl). It is a sufficient distance for changes in the universe to occur, as it covers a large part of the universe. The second method was distance modulus, which is the difference between apparent and absolute magnitudes. Based on the different measurement methods, the equations that contain the distance factor were applied twice, and a comparison was made between their results.

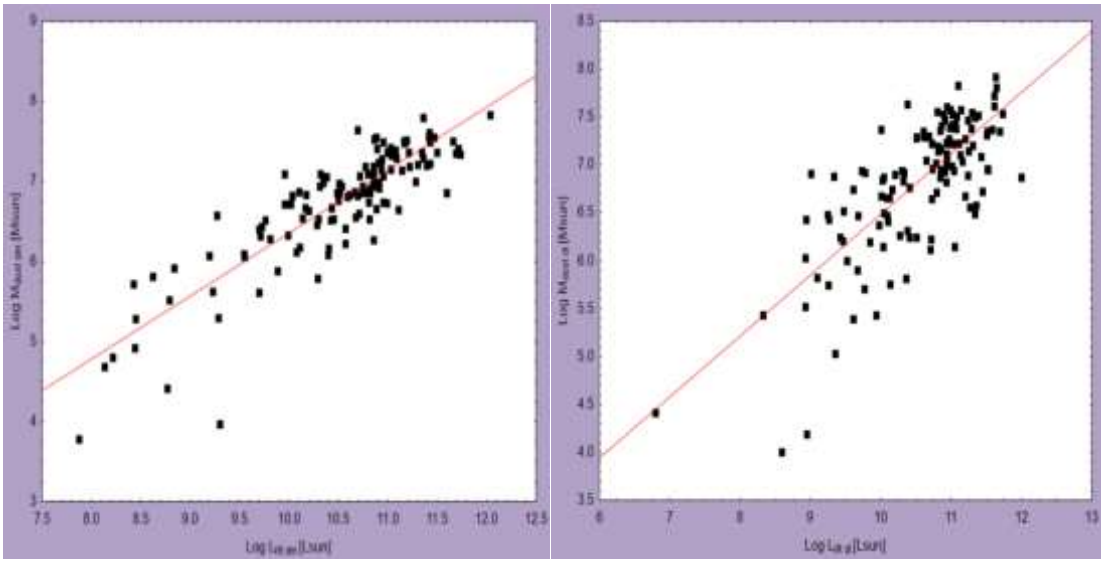

Figure 1 (a): The relation between (Log $L_{IR\ dm}$) and (Log $M_{dust\ dm}$). **Figure 1-b:** The relation between (LogL_{IRdl}) and (Log $M_{dust\ dl}$)

Figure 1 depicts the relationship between the total infrared luminosity and the mass of dust using the two methods of measuring the luminosity distance (equations 9 and 10). In Figure (1a) on the left, after the data was analyzed through the statistical program, the results show that it is a strong relationship, with a partial correlation coefficient ($R \simeq 0.7$), a high probability ($p \leq 10^{-7}$), and the slope is linear $\simeq 0.7$. As for Figure (1b) on the right, it's a good relationship,

it has a positive correlation (R≃0.6), a high probability ($p \leq 10^{-7}$), and the slope is linear≃ (0.9).

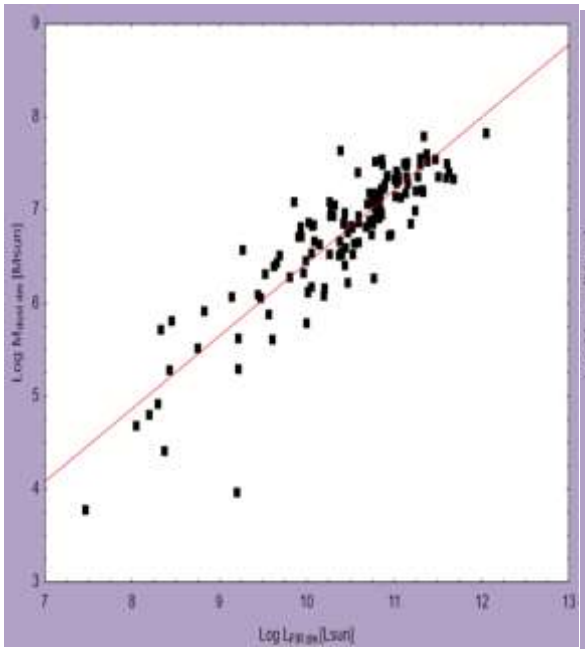

Figure 2 a: The relation between ($LogL_{FIRdm}$)& ($Log\ M_{dust\ dm}$)

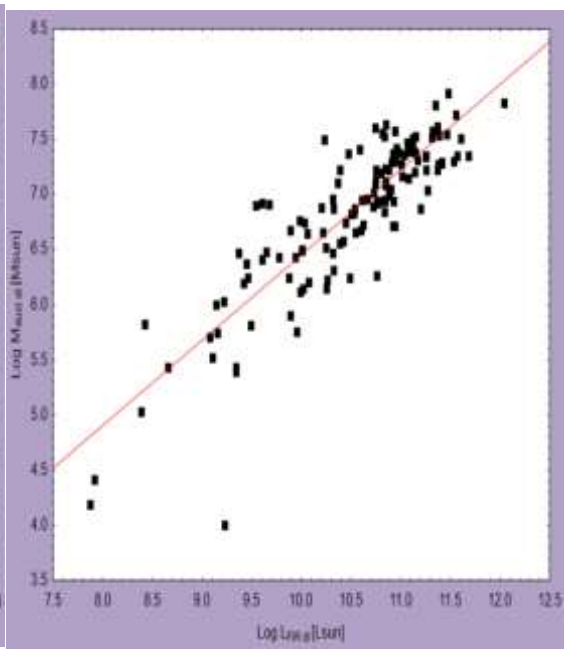

Figure 2 b:The relation between ($Log\ L_{FIRdl}$) & ($LogM_{dust\ dl}$)

Figure 2 shows how the log total infrared luminosity ($Log\ L_{FIR}$) and the log mass of dust ($LogM_{dust}$) are related. The figure on the left shows that the relationship is very good where the correlation is equal to (R≃0.7), the probability is also high ($p \leq 10^{-7}$), and the slope is linear 0.7. The figure on the right shows a good relation; it has a strong correlation (R≃0.7), very good probability ($P \leq 10^{-7}$), and the slope is linear ≃0.6. From Figures1and 2, and after comparing between them, the result is very close within all bands and with the two different methods of measuring distance. The relationship in the two figures is considered strong, as the partial correlation coefficient is very close, its percentage ranges between (0.6 - 0.7), and the slope in all figures is linear. We conclude from this that the opacity rate is very high in the luminous infrared galaxies compared to other less bright galaxies. All the results that we obtained show us several things, including the nature of the relationship between the dust mass and the luminous infrared radiation, which was determined to be a strong relationship, and the reason for making infrared telescopes, as it is known that dust constitutes approximately 1% of the astral medium and that planets and stars consist of a group of clouds of dust and gas. These clouds lead to a lack of vision for the observer, and the high correlation between the mass of dust and the bright infrared rays shown led to the trend of manufacturing telescopes that operate on the principle of infrared radiation, such as the James Webb and IRAS telescopes, because they penetrate this dust and allow us to see what is inside the galaxies and look through them into the past.

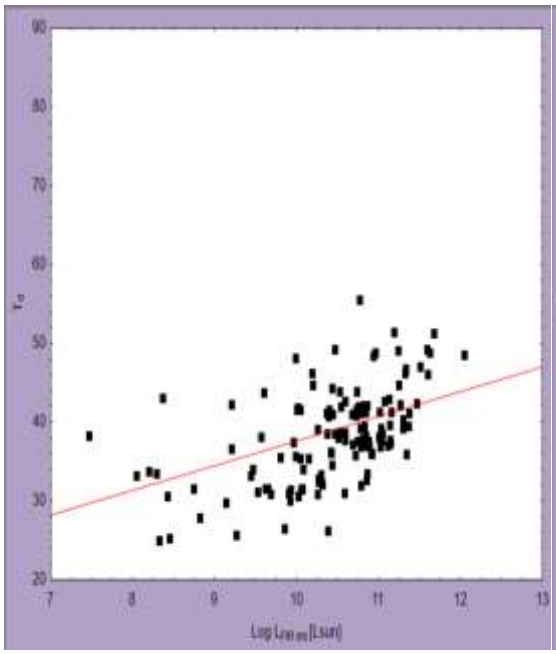

Figure 3 a: The relation between (Log $L_{FIR\ dm}$) and (T_d).

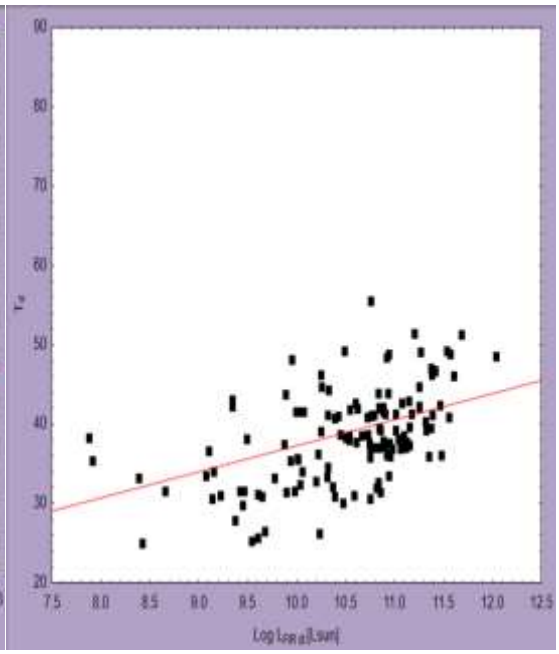

Figure 3 b: The relation between (Log$L_{FIR\ dl}$) and (T_d).

Figure 3 displays the relationship between far-infrared luminous (L_{FIR}) in solar units and dust temperature (T_d) in kelvin. The figure on the left refers to a positive relation, where the correlation is equal to($R \backsimeq 0.4$), the probability is high ($p \leq 2.2*10^{-5}$), and the slope is linear (0.6).The figure on the right shows a similar positive relation. The correlation is ($R \backsimeq 0.4$), the probability is high ($p \leq 9*10^{-6}$), and the slope is linear (0.6).

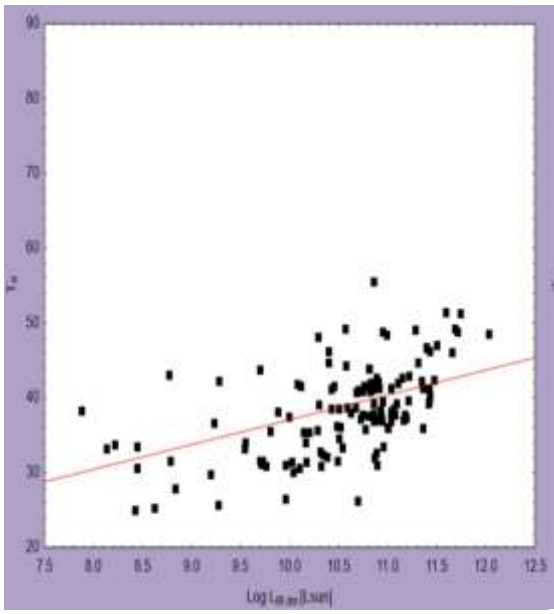

Figure 4 a: The relation between (Log $L_{IR\ dm}$) and (T_d).

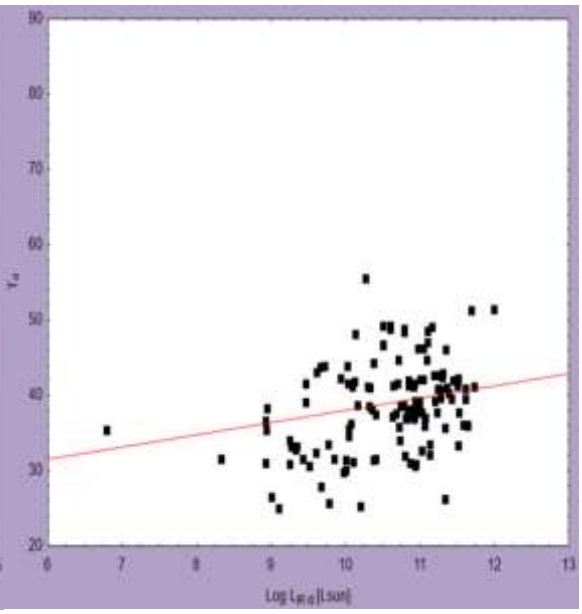

Figure 4 b: The relation between (Log $L_{IR\ dl}$) and (T_d).

The relation between total luminous infrared (L_{IR}) and dust temperature (T_d) is demonstrated in Figure 4. Figure (4a) on the left depicts a positive relation, the correlation coefficient is equal to ($R \backsimeq 0.4$), the probability is high ($p \backsimeq 2*10^{-6}$), and the slope is linear (0.7). On the right, the relation is weaker, where the correlation is ($R \backsimeq 0.2$), the probability is (0.7),

and the slope is (0.5). After obtaining the results, as shown above in Figures (3 and 4), we notice that the results of the correlation of the luminous far-infrared with the temperature of the dust in Figure (3) are very close and even equal, as the partial correlation coefficient is equal to 0.4 in both cases and that the slope is linear. Still, in Figure (4), we note that there is a difference in the results between the two types of distance, in the modulus distance (dm), it has a good correlation coefficient, as it is approximately 0.4. Yet, in the figure on the right (luminosity distance), we notice that the relationship is very weak. It is important to know how this relationship works to understand the relationship between bright infrared emissions and star formation in galaxies. These formation regions raise the temperature of the dust to obtain infrared emissions and the two most important sources for heating this dust are the general interstellar radiation field and the most intense radiation in stars. After comparing the results we obtained with previous research and studies, we found that there is a convergence in the results, as studies indicated that spiral galaxies have temperatures ranging between (30-50) Kelvin, which is almost the rate the asymptotic that we obtained in our study, which ranges between (21-51) Kelvin.

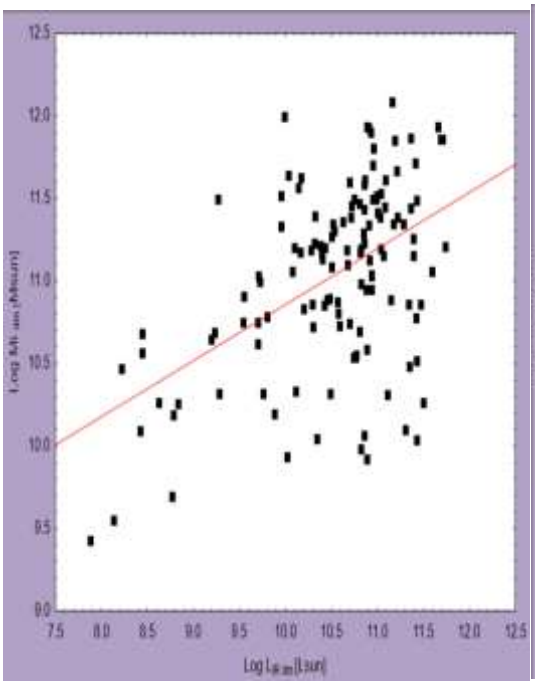

Figure 5 a: The relation between (Log $L_{IR\ dm}$) and (Log $Mi_{\ dm}$)

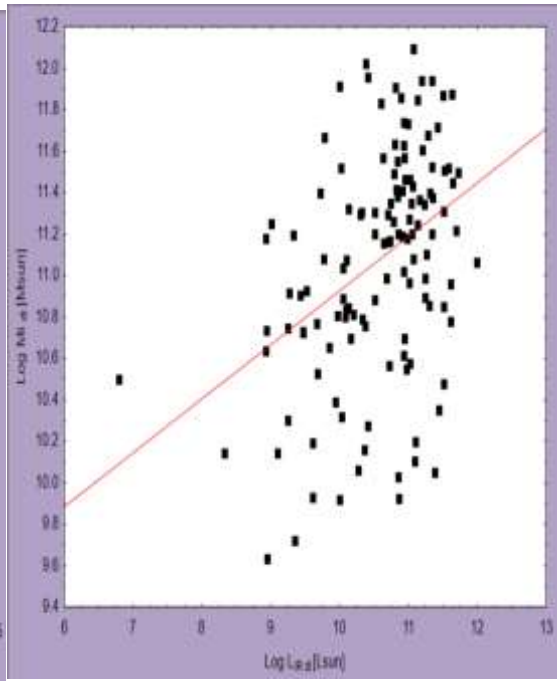

Figure 5 b: The relation between (Log $L_{IR\ dl}$) and (Log $Mi_{\ dl}$)

Figure 5 illustrates the relation between total mass (Log Mi) and the total infrared luminosity (Log L_{IR}). The figure on the left shows a positive relationship, where the correlation is ($R \simeq 0.3$), probability is ($P \simeq 1.6*10^{-3}$), and the slope is linear (0.5). The figure on the right shows a positive relationship. The correlation is ($R \simeq 0.3$), with a probability of ($2*10^{-3}$), and the slope is linear (0.5).

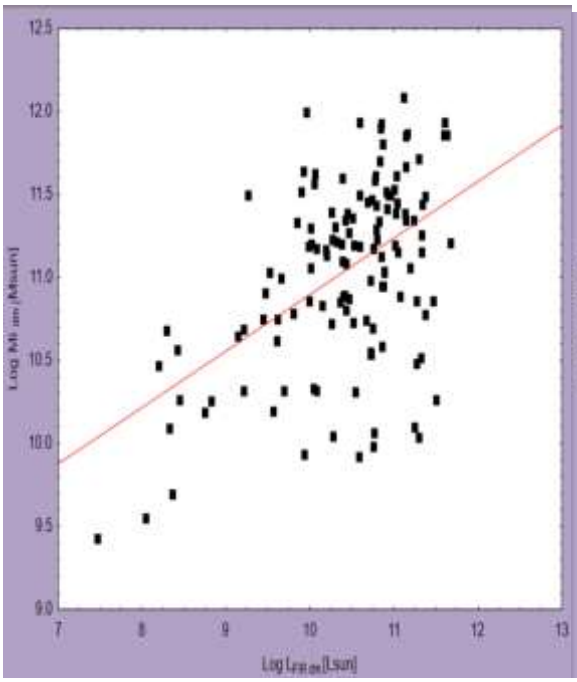

Figure 6 a: The relation between (Log $L_{FIR\ dm}$) and (Log $Mi_{\ dm}$)

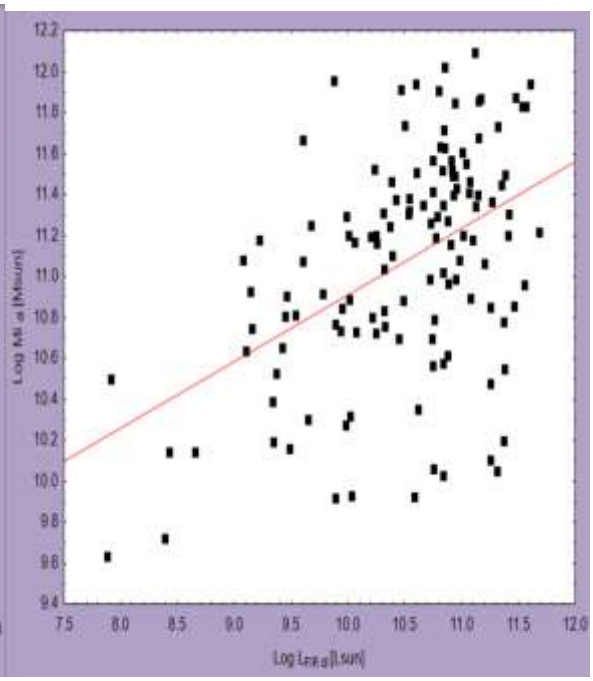

Figure 6 b: The relation between (Log $L_{FIR\ dl}$) and (Log $Mi_{\ dl}$)

Figures (6a and 6b) refer to the relation between luminous far-infrared (Log L_{FIR}) and Log total mass (Log Mi). The figure on the left shows a positive relationship, where the correlation is ($R \simeq 0.4$), the probability is ($p \simeq 7*10^{-6}$), and the slope is linear (0.5). The figure on the right is good, the correlation is equal to ($R \simeq 0.4$), the probability is equal to ($p \simeq 2.5*10^{-5}$), and the slope is linear (0.5). Through Figures (5 and 6), we notice that the relationships are positive in all cases of distance, and this indicates that the total visible mass of galaxies increases with the increase of luminous infrared emissions because these galaxies are giant galaxies in terms of their total mass, where the correlation coefficient ratio is close. The slope is linear in all cases.

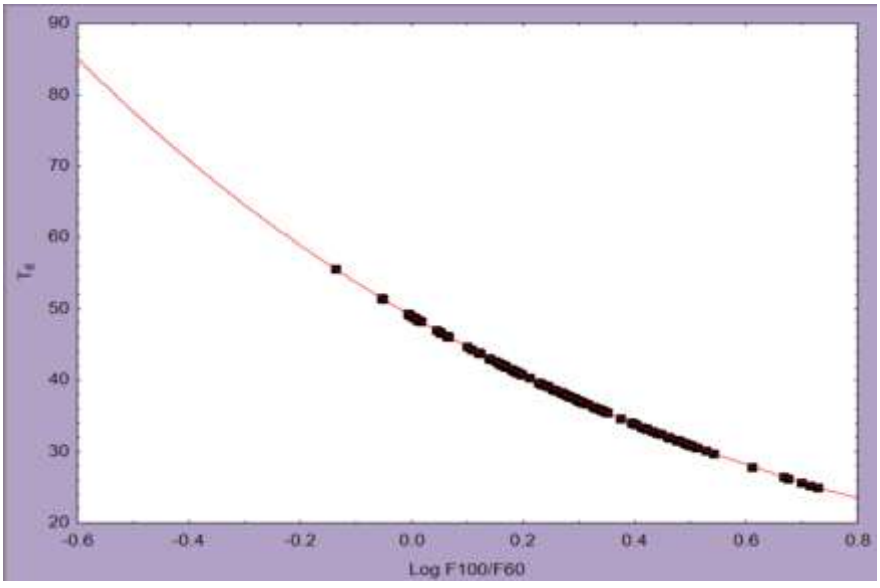

Figure 7: The relation between (Log F_{100}/F_{60}) and (T_d)

The reversal relationship shown in Figure 7 above has a partial correlation value of ($R \backsimeq - 0.9$) between the logarithm flux (100/60) and dust temperature, with a high probability of ($p \leq 10^{-7}$) and a slope of (-1).

5. Conclusion

There are different correlations for far and total luminous infrared radiation; according to the results of the statistical analysis program, it was a positive linear relationship with a high correlation coefficient ($R \backsimeq 0.7$) between the Logarithm of dust mass (M_{dustdm}&M_{dustdl}) and luminous infrared (L_{FIRdm}, L_{IRdm}) and (L_{FIRdl}, L_{IRdl}).This is due to the fact that this type of galaxy contains more dust than other types that are less bright, but despite that the luminous infrared rays have the ability to penetrate the dust and pass through it.The relationship between (L_{FIR}) and (T_d) was positive and linear, but when associated with total-infrared, the nature of the association was positive with (L_{IRdm}) and the association was weak in the case of (L_{IRdl}), where the correlation was ($R \backsimeq 0.2$). We have found that the temperature of the dust is associated with the process of star formation, as most of the luminous infrared galaxies are characterized by large masses, and therefore the larger the masses, the lower the temperature, and this leads to a decrease in the activity of the star formation process. As for the nature of the relationship between the total mass and the luminous infrared radiation, it was a positive linear relationship in both cases (L_{FIRdm}, L_{IRdm}) and (L_{FIRdl}, L_{IRdl}). This is due to the fact that they are giant galaxies, while the nature of the relationship between the Logarithm of flux (60,100) and the dust temperature (T_d) was an inverse relationship and the correlation coefficient was equal to ($R \backsimeq -0.9$).

6. ACKNOWLEDGMENTS

We extend our thanks and sincere gratitude to all of the organizers of the NASA/IPAC Extragalactic Database (NED) and the French website Lyon-Meudon Extragalactic Database (HYPERLEDA), from which the data in this research have been collected, and to all of the people who taught us.

References

[1] D.B. Sanders and I. F. Mirabel, "Luminous Infrared Galaxies", *Astron. Astrophys*, vol.792, pp:750-786,1996.

[2] F. Casoli, J. Lequeux, and F. Davd , "Infrared Space Astronomy Today and Tomorrow " ,*Cooperation With the NATO Scientific Affair Division*, vol.375, pp:343-352, 1998.

[3] J. M. Martin, L. Bottinelli, M. Dennefeld ,and L.Gouguenheim, "An 18-cm OH and 21-cm HI Survey of Luminous Far-Infrared Galaxies II.HI Proprties ", *Astron. Astrophys*, vol.245, pp:393-417, 1991.

[4] C. Cao , H. Wu , J. L.Wang, C. N. Hao, Z. G. Deng, X. Y. Xia, and Z. L. Zou, "A Catalog of Luminous Infrared Galaxies in the IRAS Survey and the Second Data Release of the SDSS ",Chin. J. *Astron. Astrophys*, vol. 0 (200x), pp:2-14, 2005.

[5] A. G. Tekola, P.Vaisanen, and A. Berlind ,"The Environments of Local Luminous Infrared Galaxies Star Formation Rates Increase With Density", vol.419,pp: 1176–1186, 2012.

[6] A. Psychogyios, V. Charmandaris, T. Diaz- Santos, L. Armus, S. Haan, J. Howell, E. Le Floc'h, S. M. Petty, and A. S. Evans, "Morphological Classification of Local Luminous Infrared Galaxies ", *Astronomy & astrophysics*, vol.591, pp: 1-16,2016.

[7] M. N. Al Najm, "Studying the Atomic and Molecular Hydrogen Mass(MHI,MH_2)Properties of the Extragalactic Spectra ", *Iraqi Journal of Science*, vol.61, no.5, pp:1233-1243, 2020.

[8] L. Colina, J. P. Lopez, S. Arribas, R. Riffel, R. A. Riffel, A. Rodriguez-Ardila, M. Pastoriza, T. Storchi-Bergmann, A. Alonso-Herrero, and D. Sales,"Understanding the Two-Dimensional Ionization Structure in Luminous Infrared Galaxies ", *Astronomy&Astrophysics*, vol.578, pp:1-19, 2015.

[9] D. A. Dale, G. J. Bendo, C. W. Engelbracht, K. D. Gordon, M.W. Regan, L. Armus, J. M. Cannon, D. Calzetti, B.T. Draine, G. Helou, R. D. Joseph, R. C. Kennicutt, A. Li, E. J. Murphy, H. Roussel, F. Walter, H. M. Hanson, D. J. Hollenbach, T.H. Jarrett, L. J. Kewley, C. A. Lamanna, C. Leitherer, M. J. Meyer, G. H. Rieke, M. J. Rieke, K. Sheth, J. D. T. Smith, and M. D. Thornley, "Infrared Spectral Energy Distribution of Nearby Galaxies ".*The Astrophysical Journal*, vol 633, pp:857-870, 2005.

[10] H. R. Schmitt, R. R. Antonucci, J. S. Ulvestad, A. L. Kinney, C. J. Clarke, and J. E. Pringle, "Testing the Unfied Model with an Infrared Selected Sample of Seyfert Galaxies ",*The Astrophysical Journal*, vol.555, pp:663-672, 2001.

[11] A. Alonso-Herrero, M. Pereira-Santaella, G. H. Rieke, and D. Rigopoulos, "Local Luminous Infrared Galaxies. II. Active Galactic Nucleus Activity from Spitzer Infrared Spectrograph Spectra",*The Astrophysical Journal*, vol.744 , pp:18, 2012.

[12] R. Riffel, A. Rodriguez-Ardila, M. S. Brotherton, R. Peletier, A. Vazdekis, R. A. Riffel, L. P. Martins, C. Bonatto, N. Z. Dametto, L. G. Dahmer-Hahn, J. Runnoe, M. G. Pastoriza, A. L. Chies-Santos, and M. Trevisan, "Optical NIR Stellar Absorption and Emission-line Indices from Luminous Infrared Galaxies ",*Advansing Astronomy and Geography*, vol.486, pp:3228–3247, 2019.

[13] M. S. Yun , N. A. Reddy, and J. J. Condon, "Radio Properties of Infrared-Selected Galaxies in The IRAS 2 Jy Sample",*The Astrophysical Journal*, vol.554, pp:803-822, 2001.

[14] X. Ma, C. C. Hayward, C. M. Casey , P. F. Hopkins , E. Quataert, L. Liang , C. A. Faucher-Giguere, R. Feldmann, and D. Keres, "Dust Attenuation ,Dust Emission, and Dust Temperature in Galaxies at $z \geq 5$ a View from the FIRE-2 Simulations ", *Advansing Astronomy and Geography*, vol.487, pp:1844–1864, 2019.

[15] D. Makarov, P. Prugniel, N. Terekhova, H. Courtois,and I. Vauglin," HyperLEDA. III. The Catalogue of Extragalactic Distances",*Astronomy &Astrophysics*, vol.570, pp:1-12, 2014.

[16] J. M. Mazzarella, and NED Team "Using the NASA /IPAC Extragalactic Database(NED) and Federated Virtual Observatory Archives for Multiwavelentgh Studies of AGNs"*ASP Conference Series*, vol.284, pp:379-388, 2002.

[17] S. Hocuk, L.Szucs, P. Caselli, S. Cazaux, M. Spaans, and G. B. Esplugues, "Parameteizing the Interstellar Dust Temperature",*Astronomy&Astrophysics*, vol.604, pp:17, 2017.

[18] D. K. Abood, and M .N. Al Najm, "Investigation of the Characteristics of CO (1-0) Line Integrated Emission Intensity in Extragalactic Spirals ",*Iraqi Journal of Science*, vol.63, pp: 1376-1394, 2022.

[19] S. H. Ali, and S .A. Albakri, "BVR CCD Photometric Observation Analysis of Spiral Galaxy Ic 467 ",*Iraqi Journal of Physics*, vol.12, pp: 81-86, 2014.

[20] M. N. Al Najm, O. Polikarpova, and Yu.Shchekinov, "Ionized Gas in the Circumgalactic Vicinity of the M81 Galaxy Group", *Astronomy Reports*, vol.60(4), pp: 389–396, 2016.

[21] R. C. Gotame, "Rotation Curve Method for Determining the Mass of Spiral Galaxies ",*Physics feed*, 2020.

[22] H. Shapley," On the Linear Diameters of 125 Large Galaxies ",*Astrophysics Journal*, vol.19, pp:1001-1006, 2018.

[23] M. Yanoff, and J. S, Duker, "Ophthalmology", *Mosby Elsevier*, pp:54,2009.

[24] P. K. Heider,"The Mean Plane of the Solar System Passing Through the Barycenter",*Wayback Machine*, vol.543, pp:11, 2013.

[25] A. Unsold, and B. Baschek, "The New Cosmos ",*Springer-Verlag Berlin Heidelberg New York*, pp:178, 2002.

[26] D. C. Agrawal, "Apparent and Absolute Magnitudes of Stars ",*An International Scientific Journal*, vol.96, pp:120-133, 2018.

[27] L. Zaninetti, "Sparse Formulae for the Distance Modulus in Cosmology ",*International Journal of Astronomy and Astrophysics*, vol.7, pp:1-22, 2021.

[28] W. L. Freedman, and B. F. Madore, "The Hubble Constant ",*Astron.Astrophysics*,vol.48,pp: 673–710,2010.

[29] Y. E. Rashed, J. Zuther, A. Eckart, G. Busch, M. Valencia-S., M. Vitale, S. Britzen, and T. Muxlow, " High-resolution Observations of SDSS J080800.99+483807.7 in the Optical and Radio Domains A possible Example of Jet-triggered Star Formation", A.&A. vol. 558, A5 , 2013.

[30] P. J. Elahi, H. S. Mahdi, Ch. Power and G. F. Lewis, " Warm Dark Haloes Accretion Histories and their Gravitational Signatures", *Monthly Notices of the Royal Astronomical Society*, vol. 444, Issue 3, pp:2333–2345, 2014.

[31] E. Robert, "The Distinction is Made Clear in Harrison ",*Cambridge University Press*, vol.59, pp:306, 2000.

[32] H. A. Abd-Al-Lateef ,and H. S. Mahdi, "The Dependence of The Gravitational Lensing Properties on The Lens And Source Redshifts " ,*Iraqi Journal of Science*, vol.63, pp:866-876, 2022.

[33] A. K. Ahmed,"Comparison of the Structure of Spiral and Lenticular Galaxies,NGC 4305 and NGC4203 as a Sample",*Iraqi Journal of Science* ,vol.64, pp:2051-2059, 2023.

[34] H. R. Al-baqir, A. K. Ahmed, and D. Gamal," Surface Photometry of NGC 3 Lenticular Galaxy",*Iraqi Journal of Science*, vol.60, pp: 2080-2086, 2019.

[35] M. N. Al Najm, Y. E. Rashed and H. H. AL-Dahlaky**, "**Spectral Multi-Wavelength Properties of a RBSC-NVSS Observation for a Sample of Active Galaxies", *Indian Journal of Natural Sciences*, vol. 9(51), pp: 15729-15740, 2018.